

## Compensation of Utility Current and Supply Power to Non-Linear Load by Using Fuzzy Based PV-Active Power Filter

**Mr.G. Siddartha**

PG Scholar

Department of EEE,

Chaitanya Bharathi Institute of Technology.

**Mr.Y.Praveen Kumar Reddy, M.Tech**

Associate Professor,

Department of EEE,

Chaitanya Bharathi Institute of Technology.

### ABSTRACT

*In this paper, a three-phase three-wire system, as well as a detailed PV generator, dc/dc boost converter to extract maximum radiation power using maximum power point tracking, associate degree dc/ac voltage source converter to act as an APF, is presented. A source is said to be renewable if there's no obvious limit on its availability. It may be used over and over again because it continues to replace itself. Sunshine, wind and water from rain are so renewable. sustainable resource use is that meets our present needs without compromising the power of future generations to satisfy their needs. The photovoltaic (PV) generation is more and more popular these days, while typical loads need additional high-power quality. Basically, one PV generator supply to nonlinear loads is desired to be integrated with a function as an active power filter (APF). The instantaneous power theory is applied to design the PV-APF controller, that shows reliable performances. Here fuzzy logic is used for controlling compared to other controllers. The MATLAB/SimpowerSystems tool has proved that the combined system will at the same time inject maximum power from a PV unit and compensate the harmonic current drawn by nonlinear loads.*

**INDEX TERMS** Active power filter (APF), instantaneous power theory, photovoltaic (PV), power quality, renewable energy.

### INTRODUCTION

Now a days renewable energy resources are going on increasing due to power demand and decreasing of the fossil fuels. And also the requirement of power quality is very essential concern along with power quality. The

grid-connected photovoltaic (PV) generator has today become more popular because of its reliable performance and its ability to come up with power from clean energy resources. The dc output voltage of PV arrays is connected to a dc/dc boost converter using a most power point tracking (MPPT) controller to maximize their produced energy. Then, that converter is coupled to a dc/ac voltage source device (VSC) to let the PV system push electric power to the ac utility. The local load of the PV system can specifically be a nonlinear load, such as computers, compact fluorescent lamps, and plenty of different home appliances, that needs distorted currents. Development of a method to compensate the distribution system harmonics is equally urgent. during this case, PV generators should provide the utility with distorted compensation capability, that makes currents injected/absorbed by the utility to be sinusoidal. Therefore, the harmonic compensation function is realized through flexible control of dc/ac VSC. instantaneous power theory has successfully completed active power filter (APF) designing with good performance. However, the PV-APF combination has simply been gradually developed for several years. this combination is capable of simultaneously compensating power factor, current imbalance, and current harmonics, and also of injecting the energy generated by PV with low total harmonic distortion (THD). Even once there is no energy available from PV, the combination will still operate to enhance the power quality of the utility. After that, the control techniques are improved in some later efforts to develop PV inverters with real power injection and APF features. However, their research did not show consistent results obtained by their projected theories, and they are applicable for a single-phase PV only.

The PV-APF system helps the utility supply a unity power issue and pure curved currents to the local nonlinear loads by generating the oscillating and imaginary components. once there's an excess power, that PV unit can only inject average power to the utility. As a result, this system is considered as a distributed APF, which is a better solution than adopting passive filters or centralized APFs. the most contributions of this paper are threefold.

- 1) For the first time, a fully complete PV-APF combination system is presented.
- 2) The controller based on instantaneous power theory and instantaneous power balance is proposed to replace the conventional dq-current controller for a PV unit.
- 3) Flexible operation modes of the PV-APF combination system are possible in the proposed model. The rest of this paper is organized as follows. Section II briefly introduces the implemented PV-APF combination system with the PV modeling technique and the selected MPPT topology. Section III describes the instantaneous power balance among the parts of the system mentioned in Section II. Section IV explains the proposed controller. Section V evaluates the performance of the proposed method based on simulated test cases in the MATLAB/SimpowerSystems environment. Finally, the conclusion is drawn in Section VI.

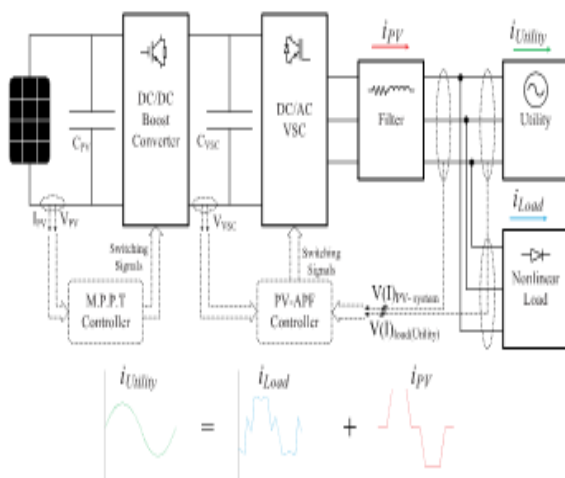


**FIGURE 1. Proposed design of PV-APF combination.**

## II. PV-APF COMBINATION SYSTEM

The PV-APF configuration is shown in Fig. 1, which consists of the following.

- 1) The PV 5series-66parallel array, which is SunPower SPR-305-type, delivers a maximum of 100-[kW] power at 1000-W/m<sup>2</sup> solar irradiance, assuming that there is no battery energy storage system connected to the dc bus.
- 2) A 5-kHz boost dc/dc converter implements MPPT by an incremental conductance–integral regulator technique, that automatically varies the duty cycle so as to generate the desired voltage to extract maximum power.
- 3) The dc bus is connected to a two-level three-phase dc/ac VSC with a CVSC capacitor. The dc/ac VSC converts the 500 [V] dc to 260 [V]/60 [Hz] ac supplying to local nonlinear loads and connects to a stiff utility. The dq-current and PV-APF and APF controllers square measure applied for this dc/ac VSC afterward.
- 4) A 10-kVAr capacitor bank filters out switching harmonics produced by the dc/ac VSC.
- 5) the loads include a three-phase diode rectifier supplying a current of 450 or 50 [A] at dc side and onephase diode rectifier with 50-[A] dc current connecting between phase A and phase B to create an overall unbalanced load.
- 6) This PV-APF combination system is connected on to the utility for shunt active filter implementation.

### A. DYNAMIC MODEL OF PV ARRAY

The PV array involves N strings of modules connected in parallel, and each string consists of M modules connected in series to get an appropriate power rating. The dynamic model of PV cell is shown in Fig. 2

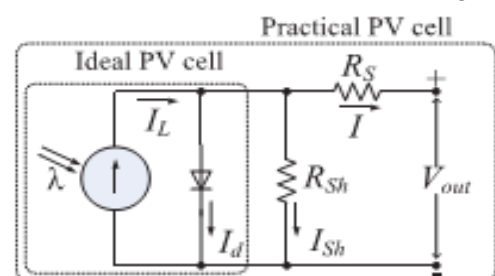


**FIGURE 2. Equivalent electrical circuit of the PV cell.**

The output-terminal current  $I$  is equal to the light-generated current  $I_L$ , less the diode-current  $I_d$  and also the shunt leakage current (or ground-shunt current)  $I_{sh}$ . The series resistance  $R_S$  represents the internal resistance to the current flow. The shunt resistance  $R_{sh}$  is inversely related to leakage current to the ground. In an ideal PV cell,  $R_S = \text{zero}$  (no series loss) and  $R_{sh} = \text{infinite}$  (no outpouring to ground). In a typical high-quality 1-in<sup>2</sup> silicon cell,  $R_S = 0.05\text{--}0.10$  and  $R_{sh} = 200\text{--}300$ . The PV conversion efficiency is sensitive to small variations in  $R_S$ , however is insensitive to variations in  $R_{sh}$ . A little increase in  $R_S$  will decrease the PV output considerably. The 2 most significant parameters mostly used for describing the cell electrical performance are the open-circuit voltage  $V_{oc} = V_{out} + R_{SI}$  obtained once the load current is zero ( $I = 0$ ) and also the short-circuit current below zero terminal voltage, the short-circuit current below this condition is that the photocurrent  $I_L$ . The basic equation describing the I-V characteristic of a practical PV cell is

$$I = I_L - I_d - I_{sh} - I_D \left[ \frac{QV_{oc}}{eAKT} - 1 \right] - \frac{V_{out} + IR_S}{R_{sh}} \quad (1)$$

where  $I_D$  is the saturation current of the diode,  $Q$  is the electron charge ( $1.6 \times 10^{-19}$  C),  $A$  is the curve fitting constant (or diode emission factor),  $K$  is the Boltzmann constant ( $1.38 \times 10^{-23}$  J/°K), and  $T$  (°K) is the temperature on absolute scale. The  $I_{sh}$ , that, in practical cells, is smaller than  $I_L$  and  $I_d$ , can be ignored. The diode-saturation current can, therefore, be determined experimentally by applying voltage  $V_{oc}$  in the dark ( $I_L = 0$ ) and measuring the current entering the cell. This current is often called the dark current or the reverse diode-saturation current  $I_d$ .

### B. MPPT IN DC/DC CONVERTER

The cell produces the maximum power at voltage corresponding to the knee point of the I-V curve, as shown in Fig. 3.  $V_{max}$  and  $I_{max}$  are voltage and current at maximum power point, respectively. The dc/dc converter is set to operate at optimal voltage to achieve maximum power by MPPT algorithm. In this paper, switching duty cycle is optimized by the MPPT

controller that uses the incremental conductance and integral regulator technique. This MPPT method is based on the fact that the power slope of the PV is null at MPP point (where  $dp/dv = 0$ ), positive in the left, and negative in the right. In the following equations,  $dv$  and  $di$  are obtained by one-sample delayed values:

$$\frac{dp}{dv} = \frac{d(vi)}{dv} = i + v \frac{di}{dv} = 0 \quad (2)$$

$$\begin{cases} \frac{dv}{di} = -\frac{i}{v} \\ \frac{dv}{di} > -\frac{i}{v} : \text{left} \\ \frac{dv}{di} < -\frac{i}{v} : \text{right} \end{cases} \quad (3)$$

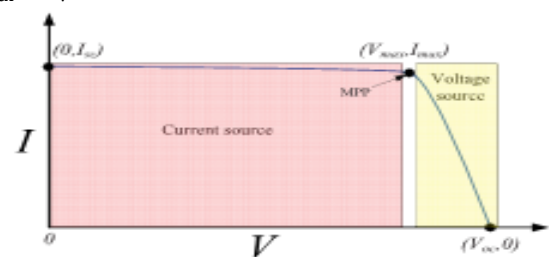


**FIGURE 3. I-V curve and remarkable points.**

The regulator output of MPPT is the duty cycle correction for semiconductor switches. In summary, the controller of the dc/dc boost converter is shown in Fig. 4.

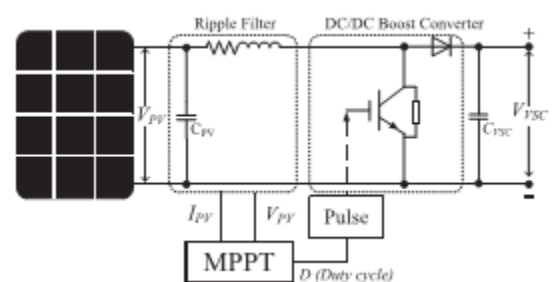


**FIGURE 4. Controller mechanism of the boost converter.**

### III. INSTANTANEOUS POWER BALANCE

Instantaneous power flow among the components of the PV-APF system simplified in Fig. 5 may be a compromise between technical constraints and designed targets. The dc/dc boost converter regulates its semiconductor switches to extract the utmost power generated by





$$\begin{cases} P_{Uti} = \bar{p}U_{ti} \\ q_{VSC} = q_L \\ p_{VSC} + p_{Uti} = P_L \\ \bar{p}_{VSC} + \bar{p}U_{ti} = \bar{p}L \\ \bar{p}_{VSC} = \bar{p}L \end{cases} \quad (6)$$

The dc/ac VSC modulates real and imaginary power balance among those parts of system.

#### IV. CONTROLLERS FOR DC/AC CONVERTER

In this section, the controllers for dc/ac VSC based on instantaneous power theory and instantaneous power balance are presented. In a conventional way, the dq-current controller is used to inject maximum real power from PV and zero reactive power to keep unity power factor of the utility. While a nonlinear load is connected close to PV position, the proposed unique PV-APF controller should be used to compensate the harmonics and help transfer the PV power. At night (no irradiance and no battery) or when there is no PV array, the APF controller is switched into the system in order to operate the CVSC capacitor just for an APF purpose.

##### PV-APF CONTROLLER

The dc/ac VSC integrated by an APF function should provide the harmonic elimination and reactive power compensation and simultaneously inject the maximum power generated by PV units. The controller is established based on the instantaneous power theory, where all the parameters are processed instantaneously. The input signals of that controller include utility voltages ( $v_{abc}$ ), nonlinear load currents ( $i_{abcL}$ ), output currents of dc/ac VSC ( $i_{abcVSC}$ ), utility injected currents ( $i_{abcUti}$ ), and dc-link voltage  $V_{VSC}$  (to prevent overcharge dc-link capacitor).

$$\begin{cases} p_L = p_{VSC} + p_{Uti} \\ q_L = q_{VSC} + q_{Uti} \end{cases} \quad (7)$$

Since the target is laid on the load, its consuming power is continuously measured and analyzed. Using the Clarke transformation, the instantaneous real power ( $p_L$ ) and imaginary power ( $q_L$ ) of the load can be calculated, as shown in the following equations:

$$\begin{bmatrix} v_\alpha(i_\alpha) \\ v_\beta(i_\beta) \end{bmatrix} = \sqrt{\frac{2}{3}} \begin{bmatrix} 1 & -\frac{1}{2} & -\frac{1}{2} \\ 0 & \frac{\sqrt{3}}{2} & -\frac{\sqrt{3}}{2} \end{bmatrix} \begin{bmatrix} v_a(i_{aL}) \\ v_b(i_{bL}) \\ v_c(i_{cL}) \end{bmatrix} \quad (8)$$

$$\begin{bmatrix} p_L \\ q_L \end{bmatrix} = \begin{bmatrix} v_\alpha & \beta \\ -v_\beta & v_\alpha \end{bmatrix} \begin{bmatrix} i_\alpha \\ i_\beta \end{bmatrix} \quad (9)$$

In general, the real and imaginary power include two parts: 1) an average (superscript  $-$ ) one, and 2) an oscillating (superscript  $\sim$ ) one, which are realized through an LPF (or rarely a high-pass filter). The LPF cutoff frequency must be selected carefully as to the inherent dynamics of loads that lead to compensation errors during transients. Unfortunately, the unavoidable time delay of the LPF may degrade the controller performance. In practice, a fifth-order Butterworth LPF with a cutoff frequency between 20 and 100 [Hz] has been used successfully depending on the spectral components in oscillating part that is to be compensated

$$\begin{cases} p_L = \bar{p}L + \bar{p}L \\ q_L = \bar{p}L + \bar{q}L \end{cases} \quad (10)$$

The average part derives from the fundamental component of nonlinear load current, while the oscillating part results from the harmonics and negative-sequence components. After successful compensation, the imaginary power and the oscillating part of the real power will come from the dc/ac VSC. The utility, in that case, supplies only one fraction of the average power required from the load. The rest is supposed to be from the PV array. In addition, the dc-link voltage regulator determines an extra amount of real power ( $p^-$  loss) that causes additional flow of energy to (from) the dc-link capacitor CVSC in order to keep its voltage around a fixed reference value ( $V_{VSCref}$ ). That real power is fed by the utility. Furthermore, the dc-link voltage regulation passes through a fuzzy-controller via the LPF, which filters out the switching harmonics existing in the dc capacitor voltage. Eventually, reference powers are

passed to a current references calculation block. These ideas make the following equations:

$$\begin{cases} \bar{p}_L + \bar{p}_L = \bar{p}_{VSC} + \bar{p}_{VSC} + \bar{p}_{Uti} + \bar{p}_{loss} \\ \bar{q}_L + \bar{q}_L = \bar{q}_{VSC} + \bar{q}_{VSC} + \bar{q}_{Uti} \end{cases}$$

$$\Rightarrow \begin{cases} \bar{q}_{VSC} = \bar{p}_L - \bar{p}_{Uti} + \bar{p}_{loss} \\ \bar{q}_{VSC} = \bar{q}_L - \bar{q}_{Uti} \\ \bar{p}_{VSC} = \bar{p}_L \\ \bar{q}_{VSC} = \bar{q}_L \end{cases} \quad (11)$$

$$\Leftrightarrow \begin{cases} p_{VSC}^{ref} = p_L - \bar{q}_{Uti} - \bar{p}_{loss} \\ q_{VSC}^{ref} = q_L - \bar{q}_{Uti} \end{cases} \quad (12)$$

If the  $p^-$  loss is supplied by the PV unit and the PV-APF combination compensates all imaginary power of load demand, (12) is changed to

$$\begin{cases} p_{VSC}^{ref} = p_L - \bar{q}_{Uti} - \bar{p}_{loss} \\ q_{VSC}^{ref} = q_L \end{cases} \quad (13)$$

After finding out the reference power for dc/ac VSC, using the reverse Clarke transformation, the reference current values in the three phases are generated as seen in the following equations:

$$\begin{bmatrix} i_{aVSC}^{ref} \\ i_{bVSC}^{ref} \\ i_{cVSC}^{ref} \end{bmatrix} = \begin{bmatrix} v_\alpha & v_\beta \\ -v_\beta & v_\alpha \end{bmatrix}^{-1} \begin{bmatrix} p_{VSC}^{ref} \\ q_{VSC}^{ref} \end{bmatrix} \quad (14)$$

$$\begin{bmatrix} i_{aVSC}^{ref} \\ i_{bVSC}^{ref} \\ i_{cVSC}^{ref} \end{bmatrix} = \sqrt{\frac{2}{3}} \begin{bmatrix} 1 & 0 \\ -\frac{1}{2} & \frac{\sqrt{3}}{2} \\ -\frac{1}{2} & -\frac{\sqrt{3}}{2} \end{bmatrix} \begin{bmatrix} i_{aVSC}^{ref} \\ i_{bVSC}^{ref} \end{bmatrix} \quad (15)$$

Fig. 6 summarizes the complete algorithm of a controller for three-phase three-wire dc/ac VSC that compensates oscillating real power and oscillating imaginary power, and supplies real power of load. The hysteresis control technique is used to switch insulated-gate bipolar transistor gates.

### APF CONTROLLER

This section reminds the topology of well-known APF controllers based on instantaneous power theory. The APF applications mentioned in [7] use this Akagi technique. The utility currents are not measured by this controller. Only the load currents and the output

currents of the APF are measured. The greatest difference of this controller compared with the PV-APF controller is the calculated reference values generated from C VSC, which are oscillating powers as in

$$\begin{cases} p_{VSC}^{ref} = \bar{p}_L + \bar{p}_{loss} \\ q_{VSC}^{ref} = \bar{q}_L \end{cases} \text{ or}$$

$$\begin{cases} p_{VSC}^{ref} = \bar{p}_L + \bar{p}_{loss} \\ q_{VSC}^{ref} = q_L \end{cases} \quad (16)$$

In this case, the utility must supply the constant dc-link voltage regulation  $p^-$  loss.

### V. FUZZY LOGIC CONTROLLER

In FLC, basic control action is determined by a set of linguistic rules. These rules are determined by the system. Since the numerical variables are converted into linguistic variables, mathematical modeling of the system is not required in FC.

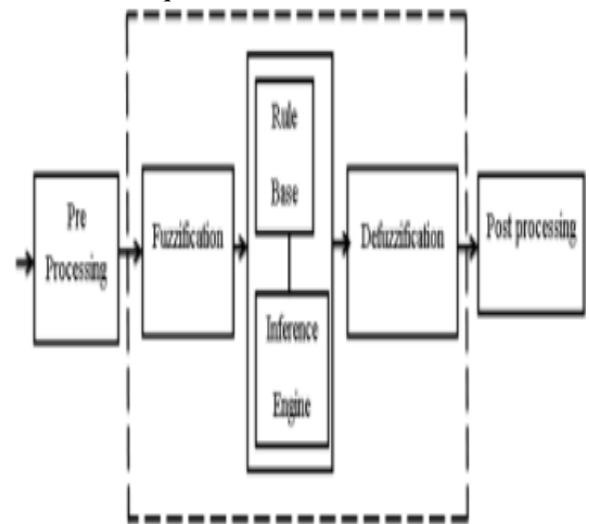


**Fig.9.Fuzzy logic controller**

The FLC comprises of three parts: fuzzification, interference engine and defuzzification. The FC is characterized as i. seven fuzzy sets for each input and output. ii. Triangular membership functions for simplicity. iii. Fuzzification using continuous universe of discourse. iv. Implication using Mamdani's, 'min' operator. v. Defuzzification using the height method.

**TABLE I: Fuzzy Rules**

| Change in error | Error |    |    |    |    |    |    |
|-----------------|-------|----|----|----|----|----|----|
|                 | NB    | NM | NS | Z  | PS | PM | PB |
| NB              | PB    | PB | PB | PM | PM | PS | Z  |
| NM              | PB    | PB | PM | PM | PS | Z  | Z  |
| NS              | PB    | PM | PS | PS | Z  | NM | NB |
| Z               | PB    | PM | PS | Z  | NS | NM | NB |
| PS              | PM    | PS | Z  | NS | NM | NB | NB |
| PM              | PS    | Z  | NS | NM | NM | NB | NB |
| PB              | Z     | NS | NM | NM | NB | NB | NB |

### Fuzzification:

Membership function values are assigned to the linguistic variables, using seven fuzzy subsets: NB (Negative Big), NM (Negative Medium), NS (Negative Small), ZE (Zero), PS (Positive Small), PM (Positive Medium), and PB (Positive Big). The Partition of fuzzy subsets and the shape of membership CE(k) E(k) function adapt the shape up to appropriate system. The value of input error and change in error are normalized by an input scaling factor.

In this system the input scaling factor has been designed such that input values are between -1 and +1. The triangular shape of the membership function of this arrangement presumes that for any particular E(k) input there is only one dominant fuzzy subset. The input error for the FLC is given as

$$E(k) = \frac{P_{ph}(k) - P_{ph}(k-1)}{V_{ph}(k) - V_{ph}(k-1)} \quad (17)$$

$$CE(k) = E(k) - E(k-1) \quad (18)$$

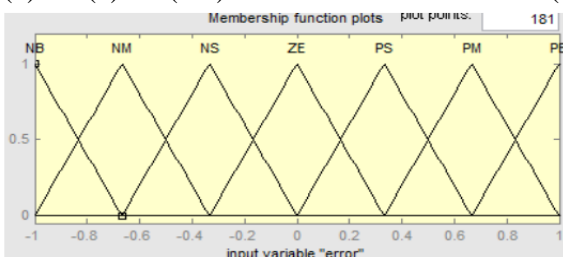


**Fig.10. Membership functions**

### Inference Method:

Several composition methods such as Max-Min and Max-Dot have been proposed in the literature. In this paper Min method is used. The output membership

function of each rule is given by the minimum operator and maximum operator. Table 1 shows rule base of the FLC.

### Defuzzification:

As a plant usually requires a non-fuzzy value of control, a defuzzification stage is needed. To compute the output of the FLC, „height“ method is used and the FLC output modifies the control output. Further, the output of FLC controls the switch in the inverter. In UPQC, the active power, reactive power, terminal voltage of the line and capacitor voltage are required to be maintained. In order to control these parameters, they are sensed and compared with the reference values. To achieve this, the membership functions of FC are: error, change in error and output

The set of FC rules are derived from

$$u = -[\alpha E + (1-\alpha)C] \quad (19)$$

Where  $\alpha$  is self-adjustable factor which can regulate the whole operation. E is the error of the system, C is the change in error and u is the control variable. A large value of error E indicates that given system is not in the balanced state. If the system is unbalanced, the controller should enlarge its control variables to balance the system as early as possible. On the other hand, small value of the error E indicates that the system is near to balanced state.

## VI. SIMULATION VALIDATION

The system in Fig. 1 is simulated in MATLAB/SimpowerSystems to test the PV-APF unit, which connects directly to the ac-utility, and to validate its ability to filter out the harmonic of nonlinear loads. The main parameters of the system used in the simulation study are indicated in Table 1. The simulation is run in a period of 0.75 s. The important time instances are: 1) at 0.05 s, turn ON MPPT and VSC dq-current controller; 2) at 0.35 s, activate MPPT; 3) at 0.5 s, switch VCS dq-current controller to PV-APF controller; 4) at 0.6 s, switch to APF controller without PV; 5) at 0.7 s, switch PV-VSC out of system; and 6) at 0.75 s, stop simulation.

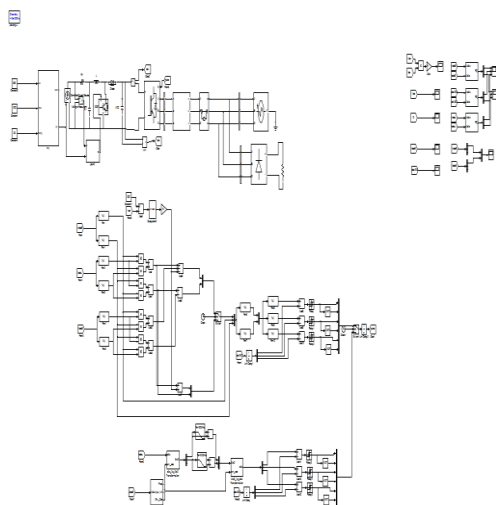


**FIGURE 6.**simulation model of proposed system

**TABLE 1.**System parameters in simulation.

|                                   |               |
|-----------------------------------|---------------|
| <b>Utility</b>                    |               |
| Voltage ( $v_{abc}$ )             | 260V          |
| Frequency ( $f$ )                 | 60Hz          |
| $R_s, L_s$                        | ideal         |
| <b>DC/AC VSC</b>                  |               |
| DC-link voltage ( $V_{DC}$ )      | 500V          |
| DC-link capacitor ( $C_{DC}$ )    | 24000 $\mu$ F |
| ShAPF filter ( $R_{AF}, L_{AF}$ ) | (0, 0.2mH)    |
| <b>Unbalanced Nonlinear Load</b>  |               |
| 3-phase diode rectifier           |               |
| Constant DC current, $I_{DC1}$    | 450A and 50A  |
| 1-phase diode rectifier           |               |
| Constant DC current, $I_{DC2}$    | 50A           |
| <b>PI-controller</b>              |               |
| ( $K_p, K_i$ )                    | (7,800)       |

## PV UNIT PERFORMANCE

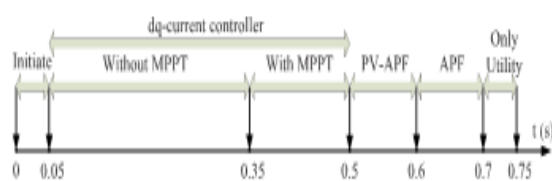


**FIGURE 7.**Operation modes of simulation.

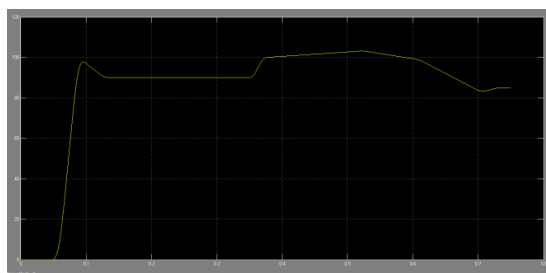
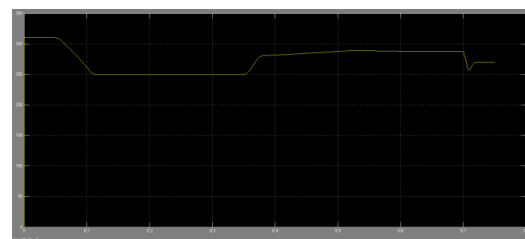
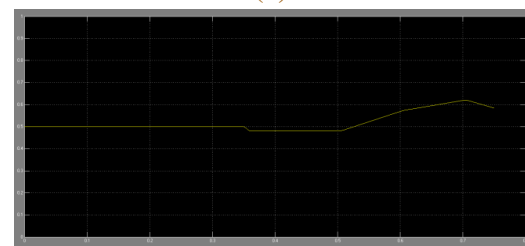


**FIGURE 8.**Output power of PV during running time.



(a)



(b)

**FIGURE 9.** Duty cycle and VPV changed by MPPT.

## Output voltage of PV unit. (b) Duty cycle of MPPT.

From 0.6 s, the duty cycle running in PV-APF mode slightly increased to adapt to power dynamic response of compensation. Because the PV unit runs in the conventional dq-current controller until 0.5 s, the power output, including 100-[kW] active power

## ACTIVE POWER FILTERPERFORMANCE

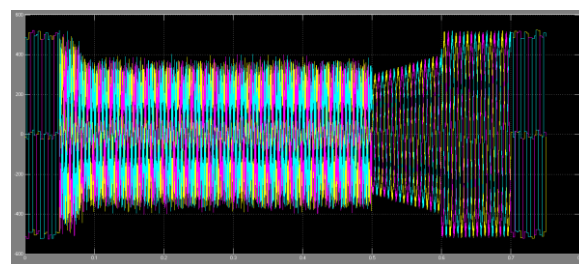


**FIGURE 10.** Utility supplied current waveform.

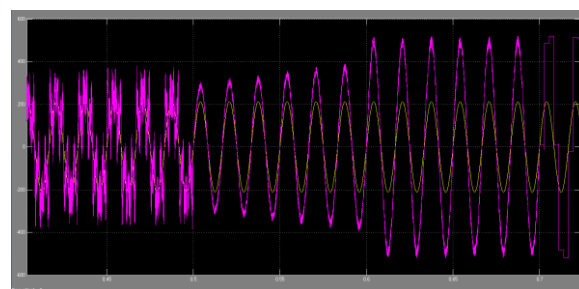
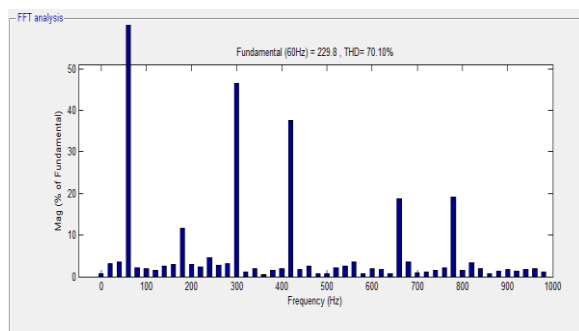
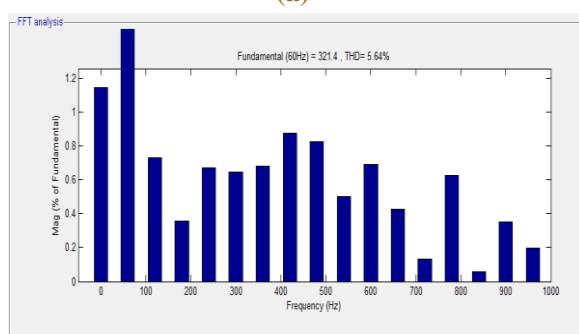


**FIGURE 11.** Utility supplied current and PCC voltage waveform.

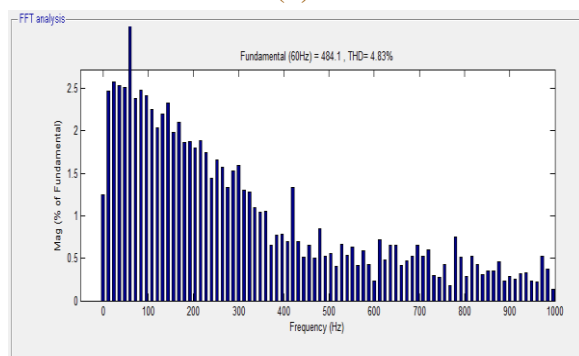




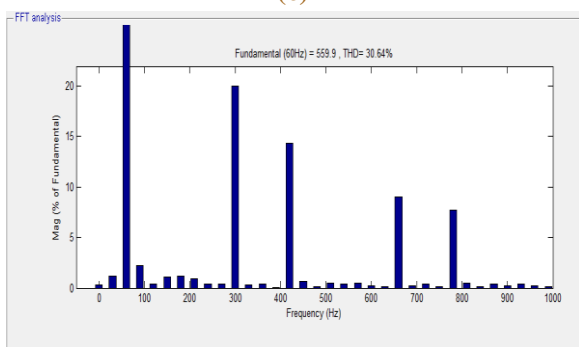
(a)



(b)



(c)



(d)

**FIGURE 12. THD in four modes of PV system operation while utility supplies power. (a) dq-current mode. (b) PV-APF mode. (c) APF mode. (d) Only utility supplies load.**

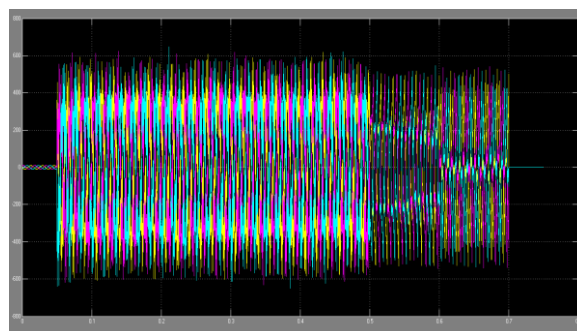


**FIGURE 13. PV supplied current waveform.**

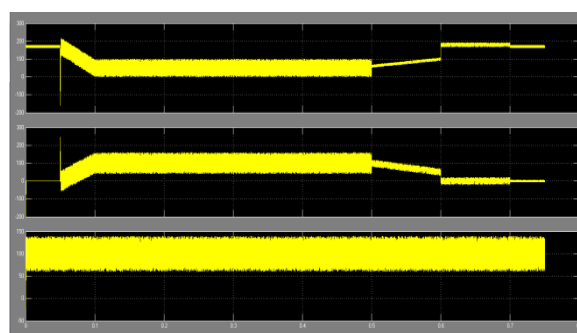


**FIGURE 14. Real power from the (a) utility, (b) PV unit, and (c) load, while the utility supplies power.**

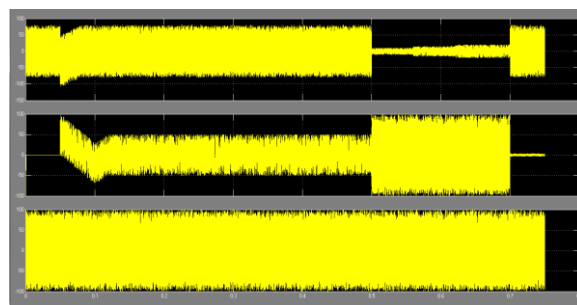


**FIGURE 15. Imaginary power from the (a) utility, (b) PV unit, and (c) load, while the utility supplies power.**

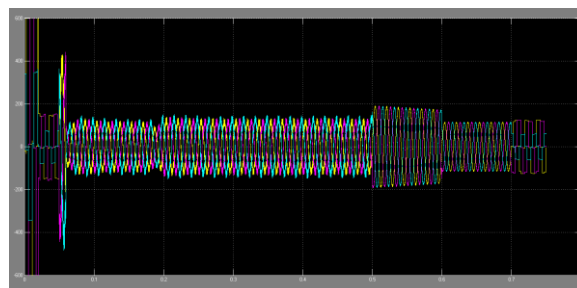
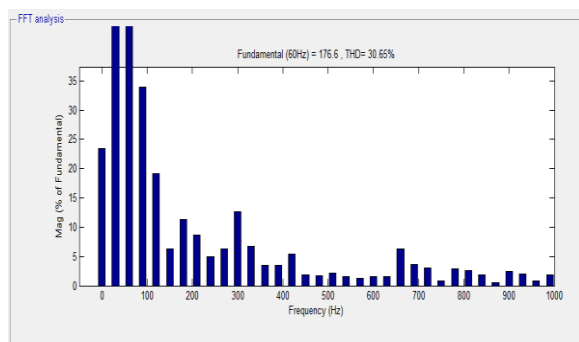
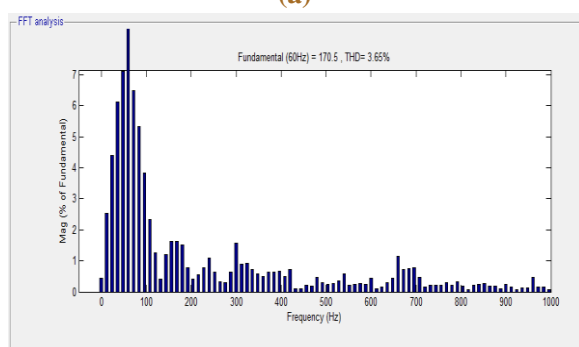


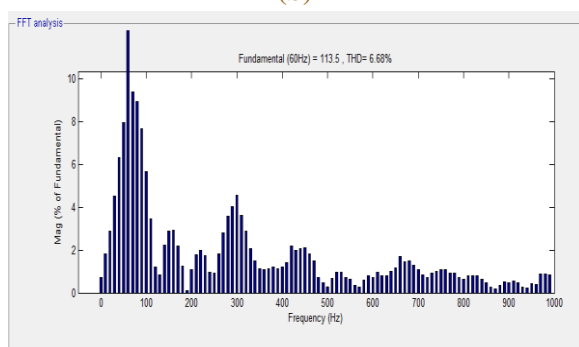
**FIGURE 16. Utility received current waveform.**



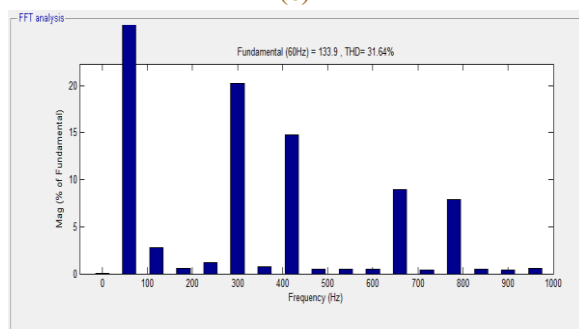
(a)



(b)



(c)



(d)

**FIGURE 17. THD in four modes of PV system operation while utility receives power. (a) dq-current mode. (b) PV-APF mode. (c) APF mode. (d) Only utility supplies load.**

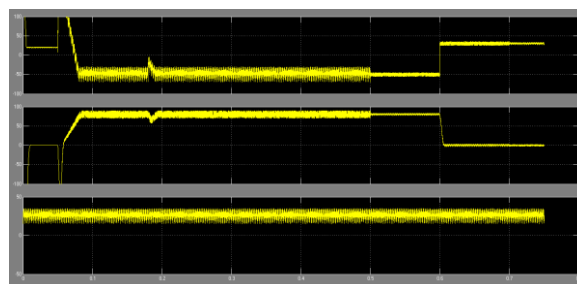


**FIGURE 18. Real power from the (a) utility, (b) PV unit, and (c) load, while the utility receives power.**

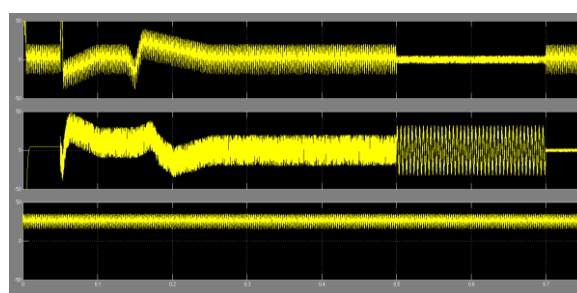


**FIGURE 19. Imaginary power from the (a) utility, (b) PV unit, and (c) load, while the utility receives power.**

## VI. CONCLUSION

In this paper, a PV-APF combination system with a local controller is proposed. To compensate the utility current without any harmonics The controller implements 2 purposes, that are activity power from the PV unit and filtering the harmonics of the local nonlinear load The new controller based on instantaneous power balance has Been explained consequently. The MATLAB/Simpower Systems simulation shows sensible performances of this controller. Here fuzzy controller is used compared to alternative controllers because of its accurate performance. The positive influence of MPPT on increasing PV power output is additionally valid. The shift among 3 controllers to dc/ac VSC brings different current waveforms. As a result, the conventional dq-current controller should not be applied once PV is connected to a local nonlinear load regarding power-quality viewpoint. whereas a PV unit is deactivated, the APF function will still operate. It is, therefore, technically possible for these power electronics-interfaced dg units to actively regulate the power

quality of the distribution system as an auxiliary service, which will certainly make those dg units extra competitive.

## REFERENCES

- [1] L. Hassaine, E. Olias, J. Quintero, and M. Haddadi, "Digital power factor control and reactive power regulation for grid-connected photovoltaic inverter," *Renewable Energy*, vol. 34, no. 1, pp. 315–321, 2009.
- [2] N. Hamrouni, M. Jraidi, and A. Cherif, "New control strategy for 2-stage grid-connected photovoltaic power system," *Renewable Energy*, vol. 33, no. 10, pp. 2212–2221, 2008.
- [3] M. G. Villalva, J. R. Gazoli, and E. R. Filho, "Comprehensive approach to modeling and simulation of photovoltaic arrays," *IEEE Trans. Power Electron.*, vol. 24, no. 5, pp. 1198–1208, May 2009.
- [4] N. R. Watson, T. L. Scott, and S. Hirsch, "Implications for distribution networks of high penetration of compact fluorescent lamps," *IEEE Trans. Power Del.*, vol. 24, no. 3, pp. 1521–1528, Jul. 2009.
- [5] I. Houssamo, F. Locment, and M. Sechilariu, "Experimental analysis of impact of MPPT methods on energy efficiency for photovoltaic power systems," *Int. J. Elect. Power Energy Syst.*, vol. 46, pp. 98–107, Mar. 2013.
- [6] M. A. G. de Brito, L. P. Sampaio, G. Luigi, G. A. e Melo, and C. A. Canesin, "Comparative analysis of MPPT techniques for PV applications," in *Proc. Int. Conf. Clean Elect. Power (ICCEP)*, Jun. 2011, pp. 99–104.
- [7] M. El-Habrouk, M. K. Darwish, and P. Mehta, "Active power filters: A review," *Proc. IEE – Elect. Power Appl.*, vol. 147, no. 5, pp. 403–413, Sep. 2000.
- [8] H. Akagi, Y. Kanagawa, and A. Nabae, "Generalized theory of the instantaneous reactive power in three-phase circuits," in *Proc. Int. Conf. Power Electron.*, Tokyo, Japan, 1983, pp. 1375–1386.
- [9] Y. W. Li and J. He, "Distribution system harmonic compensation methods: An overview of DG-interfacing inverters," *IEEE Ind. Electron. Mag.*, vol. 8, no. 4, pp. 18–31, Dec. 2014.
- [10] S. Kim, G. Yoo, and J. Song, "A bifunctional utility connected photovoltaic system with power factor correction and UPS facility," in *Proc. Conf. Rec. 25thIEEE Photovolt. Specialists Conf.*, May 1996, pp. 1363–1368.